International Journal of Engineering, Mathematical and Physical Sciences
ISSN: 2517-9934
Vol:7, No:5, 2013

An Application of the Sinc-Collocation Method to a Three-Dimensional Oceanography Model

Y. Mohseniahouei, K. Abdella, and M. Pollanen
Department of Mathematics
Trent University
Peterborough, Ontario, Canada K9J 7B8.

Abstract—In this paper, we explore the applicability of the Sinc-Collocation method to a three-dimensional (3D) oceanography model. The model describes a wind-driven current with depth-dependent eddy viscosity in the complex-velocity system. In general, the Sinc-based methods excel over other traditional numerical methods due to their exponentially decaying errors, rapid convergence and handling problems in the presence of singularities in end-points. Together with these advantages, the Sinc-Collocation approach that we utilize exploits first derivative interpolation, whose integration is much less sensitive to numerical errors. We bring up several model problems to prove the accuracy, stability, and computational efficiency of the method. The approximate solutions determined by the Sinc-Collocation technique are compared to exact solutions and those obtained by the Sinc-Galerkin approach in earlier studies. Our findings indicate that the Sinc-Collocation method outperforms other Sinc-based methods in past studies.

Keywords—Boundary Value Problems, Differential Equations, Sinc Numerical Methods, Wind-Driven Currents

I. Introduction

IN many fields of study, modelling the governing phenomena leads to a specific set of differential equations, called boundary value problems (BVPs). In most cases, deriving analytical solutions of BVPs is extremely hard or completely impossible. Therefore, various numerical methods were developed to attack these problems. Some of the well-known numerical approximations to BVPs are finite-difference method [1], finite-element method [2], [3], boundary element method [4], shooting method [5], spline method [6], and Sinc methods.

It is well-known that Sinc-based methods are dominant over other numerical methods, especially in the presence of singularities and semi-infinite domains [7]. They are also characterized by exponentially decaying errors and rapid convergence [8]. Sinc methods reduce the governing differential or integral equations to a system of algebraic equations which makes the solution easier. Sinc-based methods have been applied to diverse scientific and engineering problems comprising heat conduction [9], [10], population growth [11], inverse problems [12], [13], astrophysics problems [14], [15], medical imaging [16], elastoplastic problems [17], and oceanography [18], [19]. Very recently, the application of Sinc-Collocation approach to the telegraph equation [20] and the second type of the Painlevé equations [21] has been studied.

Corresponding author: Dr. Kenzu Abdella
e-mail: kabdella@trentu.ca
Phone: 705-748-1011 (X 7327)
Manuscript received April 9, 2013.

In general, there are two equivalent but distinct Sinc approaches: Sinc-Galerkin and Sinc-Collocation. In earlier studies, it has been evidenced that the Sinc-Collocation approach is superior to the Galerkin one regarding its simple implementation and possible extensions to more general BVPs [22].

In the past century, hydrodynamic models and their numerical solutions obtained many accomplishments. The first wind-driven current models were one-dimensional systems based on the work of Ekman [23]. Eventually two- and three-dimensional models were developed [24], [25]. To derive approximate solutions to 3D models, several numerical methods employing spectral methods [26], B-spline approach [27], Chebyshev and Legender polynomials [28] and eigenfunction approach [29] were developed. Recently, Sinc-Galerkin approaches have been applied to a 3D wind-driven current model [18], [19].

The intent of this paper is to demonstrate an application of the Sinc-Collocation technique to a steady state 3D model of wind-driven currents with a depth-dependent eddy viscosity in coastal regions and semi-enclosed seas. The model is found in the work of Winter et al. [18]. They formulated the model as a complex-valued ordinary differential equation (ODE) and applied the original Sinc-Galerkin approach to solve it. Later, Koonprasert and Bowers [19], developed a block matrix formulation for the Sinc-Galerkin technique and applied it to the same model. In this paper, we apply the Sinc-Collocation approach to the complex-valued system and compare the results with those in earlier studies and exact solutions when available.

Following the introduction, we provide a brief explanation of the model formulation in section 2. Section 3, is devoted to the Sinc-Collocation treatment that we apply to the model. In Section 4, several model problems have been used to examine the accuracy and stability of the method. Finally, in the last section we discuss the results.

II. Problem Formulation

In this section we provide a brief explanation of the model found in the work of Winter et al. [18]. We refer interested readers to [18], [19] and references there in.

To develop this model one needs to construct a right-handed coordinate system with the vertical coordinate z^* directed

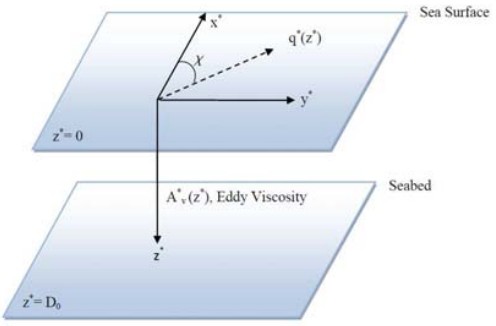

Fig. 1. A schematic description of the 3D oceanography model with depth-dependent eddy viscosity

positive downward from the free surface, and with x^* and y^* directed positive northward and eastward, respectively. We suppose that z^* changes from 0 to $D_0 = 100\ m$, and the plane at $z^* = D_0 = 100\ m$ is an impermeable boundary at the seabed [18]. This model is simplified by several assumptions. The ocean depth, D_0, and ocean mass density, ρ, are assumed constant, and the effects of tides, inertial terms, free surface slope, and variations in atmospheric pressure are neglected [18]. For a better understanding, a schematic form of the model is provided in Figure 1. Assuming τ_w as the magnitude of a tangential surface wind stress, the currents will be represented by $\tau(0) = \tau_w(\cos(\chi)\hat{x}^* + \sin(\chi)\hat{y}^*)$ where χ is the angle between the positive x^*-axis and the wind direction and $\hat{x}^*$ and $\hat{y}^*$ are unit vectors in the positive direction of x^*-axis and y^*-axis, respectively. The horizontal wind-drift current, $q^*(z^*)$, is the difference between the total velocity and the geostrophic current and given by $q^*(z^*) = U^*(z^*)\hat{x}^* + V^*(z^*)\hat{y}^*$. As well, Internal frictional stresses are parameterized as $\tau(z^*) = -\rho {A^*}_v(z^*)\frac{dq}{dz^*}$, where the specified effective vertical eddy viscosity coefficient ${A_v}^*(z^*)$ is a continuously differentiable function of $z^* \in (0, D_0)$ [18]. Considering all earlier assumptions, the wind-drift current, q^*, will be driven by solving the following BVP:

$$\frac{d}{dz^*}({A^*}_v(z^*)\frac{dq^*}{dz^*}) = -f\hat{z}^* \times q^*,\ 0 < z^* < D_0, \quad (1)$$

where the boundary conditions (BCs) are given by

$$-\rho {A_v}^*(0)\frac{dq^*(0)}{dz^*} = \tau_w\left(\cos(\chi)\hat{x}^* + \sin(\chi)\hat{y}^*\right) \quad (2)$$

$$-\rho {A_v}^*(D_0)\frac{dq^*(D_0)}{dz^*} = k_f\ \rho\ q^*(D_0) \quad (3)$$

The Coriollis parameter at latitude θ is given by $f \equiv 2\Omega\sin(\theta)$, while $\Omega = 7.29\times10^{-5}$ rad s^{-1}. Since the Coriollis force acts inversely in northern and southern hemisphere, Winter et al. [18] assumed that the sea is located in northern hemisphere, so $0 < \theta < \frac{\pi}{2}$. The parameter k_f, is defined as the linear slip bottom stress coefficient. Substituting the definition of $q^*(z^*)$ in (1), leads to

$$\frac{d}{dz^*}\left({A^*}_v(z^*)\frac{dq^*}{dz^*}\right) = -f\hat{z}^* \times q^* \quad (4)$$

$$= -f\hat{z}^* \times [U^*(z^*)\hat{x}^* + V^*(z^*)\hat{y}^*]$$
$$= -f\left(U^*(z^*)\hat{y}^* - V^*(z^*)\hat{x}^*\right).$$

which would be separated to its parts as

$$-\frac{d}{dz^*}\left({A^*}_v(z^*)\frac{dU^*(z^*)}{dz^*}\right) = -fV^*(z^*),\ 0 < z^* < D_0 \quad (5)$$

$$-\frac{d}{dz^*}\left({A^*}_v(z^*)\frac{dV^*(z^*)}{dz^*}\right) = -fU^*(z^*),\ 0 < z^* < D_0 \quad (6)$$

Similarly, the separated BCs at the sea surface, and the seabed are given by

$$-\rho {A^*}_v(0)\frac{dU^*(0)}{dz^*} = \tau_w\cos(\chi), \quad (7)$$

$$-\rho {A^*}_v(0)\frac{dV^*(0)}{dz^*} = \tau_w\sin(\chi)$$

$$\rho {A^*}_v(D_0)\frac{dU^*(D_0)}{dz^*} = k_f\rho U^*(D_0), \quad (8)$$

$$\rho {A^*}_v(D_0)\frac{dV^*(D_0)}{dz^*} = k_f\rho V^*(D_0).$$

With the help of the non-dimensional variables

$$z \equiv \frac{z^*}{D_0},\ A_v(z) \equiv \frac{{A^*}_v(z^*)}{{A^*}_v(0)}, \quad (9)$$

$$q(z) \equiv \frac{q^*(z^*)}{U_0} \equiv U(z)\hat{x} + V(z)\hat{y}$$

and non-dimensional constants, κ (depth ratio) and σ (bottom friction parameter)

$$\kappa \equiv \frac{D_0}{D_E} = D_0\sqrt{\frac{f}{2A_0}},\ \sigma \equiv \frac{A_0A_v(1)}{k_fD_0} = \frac{{A^*}_v(D_0)}{k_fD_0}. \quad (10)$$

where $A_0 \equiv {A^*}_v(0)$, $D_E \equiv \sqrt{\frac{2A_0}{f}}$, and $U_0 = \frac{\tau_w D_E}{(\rho A_0)} = \frac{\sqrt{2}\tau_w}{(\rho\sqrt{A_0 f})}$, equations (5) and (6) are transfered to non-dimensional equations

$$-\frac{d}{dz}\left(A_v(z)\frac{dU(z)}{dz}\right) = -2\kappa^2V(z),\ 0 < z < 1, \quad (11)$$

$$-\frac{d}{dz}\left(A_v(z)\frac{dV(z)}{dz}\right) = 2\kappa^2U(z),\ 0 < z < 1. \quad (12)$$

Likewise, the non-dimensionalizing procedure on BCs leads to

$$\frac{dU(0)}{dz} = -\kappa\cos(\chi),\ \frac{dV(0)}{dz} = -\kappa\sin(\chi) \quad (13)$$

$$U(1) + \sigma\frac{dU(1)}{dz} = 0,\ V(1) + \sigma\frac{dV(1)}{dz} = 0. \quad (14)$$

For the purpose of transforming the nonhomogenous BCs to homogeneous ones, the following linear transformations are applied.

$$U(z) = u(z) + \kappa(1 + \sigma - z)\cos(\chi), \quad (15)$$

$$V(z) = v(z) + \kappa(1 + \sigma - z)\sin(\chi)$$

The first derivative of the transformations are given by

$$\frac{dU(z)}{dz} = \frac{du(z)}{dz} - \kappa\cos(\chi), \quad (16)$$

$$\frac{dV(z)}{dz} = \frac{dv(z)}{dz} - \kappa \sin(\chi)$$

Hence the "reduced velocity" components $u(z)$ and $v(z)$ satisfy

$$-\frac{d}{dz}\left(A_v(z)\frac{du}{dz}\right) + \kappa\cos(\chi)A'_v(z) \tag{17}$$

$$= -2\kappa^2 v(z) - 2\kappa^3(1+\sigma-z)\sin(\chi),\ 0 < z < 1.$$

$$-\frac{d}{dz}\left(A_v(z)\frac{dv}{dz}\right) + \kappa\sin(\chi)A'_v(z), \tag{18}$$

$$= 2\kappa^2 u(z) + 2\kappa^3(1+\sigma-z)\cos(\chi),\ 0 < z < 1.$$

where the BCs at the surface and seabed are respectively given by

$$\frac{du(0)}{dz} = 0,\ \frac{dv(0)}{dz} = 0 \tag{19}$$

$$u(1) + \sigma\frac{du(1)}{dz} = 0,\ v(1) + \sigma\frac{dv(1)}{dz} = 0 \tag{20}$$

The system defined by (17)-(20) could be written in the complex-velocity system. To obtain the complex-velocity formulation, we need to multiply equation (18) by the imaginary unit i, and add the result to equation (17). Afterwards by defining a complex velocity $w(z) = u(z) + iv(z)$, we have

$$\begin{aligned}\mathcal{L}(z) &\equiv \mathcal{L}u(z) + i\mathcal{L}v(z)\\ &\equiv -\frac{d}{dz}27\left(A_v(z)\frac{du(z)}{dz}\right) - i\frac{d}{dz}\left(A_v(z)\frac{dv(z)}{dz}\right)\\ &\equiv -\frac{d}{dz}\left(A_v(z)\frac{dw(z)}{dz}\right)\end{aligned}$$

Hence the complex velocity formulation is shown by

$$\mathcal{L}w(z) - i2\kappa^2 w(z) = F(z),\ \ 0 < z < 1, \tag{21}$$

where

$$F(z) = [-\kappa A'_v(z) + i2\kappa^3(1+\sigma-z)]e^{i\chi}.$$

BCs, evolved by the same procedure, are given by

$$w'(0) = 0, \tag{22}$$

$$w(1) + \sigma w'(1) = 0. \tag{23}$$

III. The Sinc-Collocation Approach

In this section, we briefly describe a Sinc-Collocation approach via first derivative interpolation, that has been recently developed by Abdella [30]. We refer the readers to paper [30] where a comprehensive explanation of the method and Sinc preliminaries are provided.

Assume the general second-order two-point BVP:

$$a(x)y''(x) + b(x)y'(x) + c(x)y(x) = d(x),\ x \in (a,b), \tag{24}$$

$$\alpha_a y(a) + \beta_a y'(a) = \gamma_a, \tag{25}$$

$$\alpha_b y(b) + \beta_b y'(b) = \gamma_b. \tag{26}$$

where α_a, α_b, β_a, β_b, γ_a, and γ_b are constants.

The Sinc-Collocation approach introduced by Abdella [30], transforms the BVP as follows such that the BCs become homogeneous [31]:

$$u(x) = y(x) - \eta(x) \tag{27}$$

where

$$\eta(x) = y'(a)H_1 + y(a)H_2 + y(b)H_3 + y'(b)H_4 \tag{28}$$

is the univariate Hermite interpolation with the cardinal functions given by:

$$H_1 = \frac{(x-a)(x-b)^2}{(b-a)^2},\ H_2 = \frac{(x-b)^2(2x-3a+b)}{(b-a)^3},$$

$$H_3 = \frac{(x-a)^2(2x-3b+a)}{(a-b)^3},\ H_4 = \frac{(x-b)(x-a)^2}{(b-a)^2}.$$

Employing (27) and considering $\eta(a) = y(a), \eta'(a) = y'(a), \eta(b) = y(b), \eta'(b) = y'(b)$, leads to a new BVP with homogeneous BCs given by:

$$a(x)u''(x) + b(x)u'(x) + c(x)u(x) = e(x),\ x \in (a,b), \tag{29}$$

$$u(a) = u(b) = 0, \tag{30}$$

$$u'(a) = u'(b) = 0, \tag{31}$$

where

$$e(x) = d(x) - a(x)\eta''(x) - b(x)\eta'(x) - c(x)\eta(x).$$

Here is the point that our method changes its way from the original sinc-collocation technique, i.e. it first approximates $u'(x)$ at sinc points x_i by:

$$u'(x_i) = \sum_{k=-N}^{N} S(k,h)(\varphi(x_i))u'(x_k) = \sum_{k=-N}^{N} \delta_{i,k}^{(0)} u'(x_k) \tag{32}$$

Then $u(x)$ is approximated by:

$$u(x_i) = \sum_{k=-N}^{N} h_k(x_i)u'(x_k) = \sum_{k=-N}^{N} h\delta_{i,k}^{(-1)}\frac{u'(x_k)}{\varphi'(x_k)} \tag{33}$$

Finally, we can approximate $u''(x)$ via:

$$u''(x_i) = \sum_{k=-N}^{N} g_k(x_i)u'(x_k) = \sum_{k=-N}^{N} \delta_{i,k}^{(1)}\varphi'(x_i)\frac{u'(x_k)}{h} \tag{34}$$

where $\phi(x)$ is given by

$$\xi = \phi(x) = \frac{1}{\pi}\log\left(\frac{x-a}{b-x}\right) \tag{35}$$

with inverse

$$x = \psi(\xi) = \frac{b+a}{2} + \frac{b-a}{2}\tanh\left(\frac{\pi}{2}\sinh(\xi)\right) \tag{36}$$

and $x_k = \psi(kh)$. As well

$$\delta_{i,k}^{(0)} = \begin{cases} 0, & i \neq k \\ 1, & i = k, \end{cases} \tag{37}$$

$$\delta_{i,k}^{(1)} = \begin{cases} \frac{(-1)^{i-k}}{i-k}, & k \neq i \\ 0, & k = i, \end{cases} \tag{38}$$

$$\delta_{i,k}^{(-1)} = \begin{cases} \frac{1}{2} + \int_0^{i-k} \frac{\sin(\pi t)}{\pi t}, & i \neq k \\ \frac{1}{2}, & k = i. \end{cases} \tag{39}$$

Hence, the discretized version of the equation (29) will be:

$$\sum_{k=-N}^{N} M_{i,k} u'(x_k) = e(x_i) \tag{40}$$

where

$$M_{i,k} = a(x_i)\delta_{k,i}^{(1)} \frac{\varphi'(x_i)}{h} + b(x_i)\delta_{k,i}^{(0)} + c(x_i)h\frac{\delta_{k,i}^{(-1)}}{\varphi'(x_k)} \tag{41}$$

Note that (40) leads to a system of $n = 2N + 1$ equations for $(n + 4)$ unknowns including $y'(a)$, $y(a)$, $y'(b)$, $y(b)$ and $u'(x_i), i = -N, -N + 1, ..., N - 1, N$.
We define the $(n + 4) \times 1$ vector $\mathbf{C}$ by:

$$\mathbf{C} = [C_{-N-2}, C_{-N-1}, C_{-N}, ...C_0, ..., C_N, C_{N+1}, C_{N+2}]^{\mathrm{T}}$$
$$= [y(a), y'(a), u'(x_{-N})...u'(x_0), ...u'(x_N), y'(b), y(b)]^{\mathrm{T}}.$$

The four conditions required to close the system consists of the two BCs given by equations (25) and (26) and two more conditions obtained by requiring that $u(x)$ vanishes at the outside Sinc nodes $(-N - 1)$ and $(N + 1)$:

$$\alpha_a C_{-N-2} + \beta_a C_{-N-1} = \gamma_a, \tag{42}$$

$$\alpha_b C_{N+2} + \beta_b C_{N+1} = \gamma_b, \tag{43}$$

$$\sum_{k=-N}^{N} h\delta_{-N-1,k}^{(-1)} C_k = 0, \tag{44}$$

$$\sum_{k=-N}^{N} h\delta_{N+1,k}^{(-1)} C_k = 0. \tag{45}$$

The matrix representation of the $(n + 4) \times (n + 4)$ system corresponding to equations (40) and (42)-(45) is given by

$$\mathbf{AC} = \mathbf{E} \tag{46}$$

where $\mathbf{E}$, a $(n + 4) \times 1$ vector, and $\mathbf{A}$, a $(n + 4) \times (n + 4)$ matrix are given by

$$\mathbf{E} = [\gamma_a, \gamma_b, e(x_{-N}), ..., e(x_0), ..., e(x_N), 0, 0]^{\mathrm{T}},$$

$$\mathbf{A} = \begin{pmatrix} B_1 \\ B_2 \\ \mathbf{B} \\ B_3 \\ B_4 \end{pmatrix}, \tag{47}$$

where B_1, B_2, B_3 and B_4 are $1 \times (n + 4)$ matrices given by

$$B_1 = [\alpha_a, \beta_a, 0, ..., 0],$$

$$B_2 = [0, 0, ..., \beta_b, \alpha_b],$$

$$B_3 = [0, 0, h\delta_{-N-1,-N}^{(-1)}, ..., h\delta_{-N-1,N}^{(-1)}, 0, 0],$$

$$B_4 = [0, 0, h\delta_{N+1,-N}^{(-1)}, ..., h\delta_{N+1,N}^{(-1)}, 0, 0],$$

and $\mathbf{B}$ as a $n \times (n + 4)$ matrix is given by

$$\mathbf{B} = [\mathbf{0}, \mathbf{0}, \mathbf{M}, \mathbf{0}, \mathbf{0}]$$

where

$$\mathbf{0} = [0, 0, ..., 0, 0]^{\mathrm{T}}$$

is a $(n \times 1)$ vector and $\mathbf{M}$ is the $(n \times n)$ matrix format of (41).

Once equation (46) is solved, the coefficients are used to determine the unknown function $u(x)$ and its first and second derivatives at the Sinc nodes using equations (32)-(34). The original unknown, $y(x)$ is then determined from equation (27). Note also that the values of $y(x)$ and $y'(x)$ at the two end points are also determined directly from the system solutions.

IV. Numerical Illustrations

A. Constant Eddy Viscosity

In this section, we examine the accuracy of the Sinc-Collocation method in the complex velocity system while the eddy viscosity is constant. To make reliable comparisons, all the examples, parameters and variables are same as those carried out in [18], [19], [32]. For more information readers may refer to earlier studies.

Since the governing equations and variables were non-dimensionalized, the only operative constants in (21)-(23), are $\kappa = \frac{D_0}{D_E} = 5, \sigma = \frac{A^*{}_v(D_0)}{(k_f D_0)} = 0.1$, and $\chi = 45^\circ$ [18]. As well, the nominal values: $f = 0.0001$ s^{-1}, sea water density $\rho = 1 \times 10^3$ kgm^{-3}, and air density $\rho_{air} = 1.25$ kgm^{-3} are adopted. The surface wind stress given by $\tau_w = C_D \rho_{air} {W_w}^2$, is set at 0.1414 in all model problems. The linear slip bottom stress coefficient, k_f is set at 0.002 ms^{-1}. $A^*{}_v(0)$ in units of m^{2}s^{-1} is given by

$$A^*{}_v(0) \approx 0.304 \times 10^{-4} {W_w}^3 \tag{48}$$

together with the parameters and relationships above, the constant eddy viscosity is chosen to be

$$A^*{}_v(z^*) \equiv 0.02 m^2 s^{-1} \tag{49}$$

In the case of constant eddy viscosity, the exact solution is available and given by $W^*(z^*) = U_0[U(z) + iV(z)]$ where $U(z)$ and $V(z)$ are respectively represented by

$$U(z) = \mathcal{R}(W_c(z))\cos(\chi) - \mathcal{I}(W_c(z))\sin(\chi) \tag{50}$$

$$V(z) = \mathcal{R}(W_c(z))\sin(\chi) + \mathcal{I}(W_c(z))\cos(\chi) \tag{51}$$

$\mathcal{R}(W_c(z))$ and $\mathcal{I}(W_c(z))$, respectively refer to the real and imaginary parts of $W_c(z)$, where

$$W_c(z) = \frac{\kappa(1-i)\sigma\cosh(\kappa(1-i)(1-z)) + \sinh(\kappa(1-i)(1-z))}{(1-i)[\cosh(\kappa(1-i)) + \kappa(1-i)\sigma\sinh(\kappa(1-i))]} \tag{52}$$

The results of the Sinc-Collocation approach shown by $U_c(z_j)$ and $V_c(z_j)$ were compared with the exact solutions, $U(z_j)$ and $V(z_j)$, at the sinc grid points $\mathcal{S}$ with the mesh size of

$$h = \frac{\log(\pi d\gamma N/\beta)}{\gamma N}$$

TABLE I
ERRORS OF EXAMPLE 1 (CONSTANT EDDY VISCOSITY) WHILE $\sigma = 0.1, \chi = 45^\circ, \kappa = 5, D_0 = 100\ m$ AND $D_E = 20\ m$.

N	m	h	$\|E_U\|$	$\|E_V\|$	$\|E_W\|$
4	13	0.3163	2.99×10^{-3}	3.47×10^{-3}	3.47×10^{-3}
8	21	0.2015	1.26×10^{-4}	8.41×10^{-5}	1.26×10^{-4}
16	37	0.1224	2.49×10^{-6}	1.23×10^{-6}	2.49×10^{-6}
32	69	0.0720	2.96×10^{-8}	1.43×10^{-8}	2.96×10^{-8}
64	133	0.0414	1.23×10^{-10}	1.82×10^{-10}	1.82×10^{-10}

where d, γ, and β are equal to $\frac{\pi}{4}$, 2, and $\frac{\pi}{2}$ respectively. In order to provide dimensional representation of the velocities we need to multiply the results by the natural velocity scale U_0.

To demonstrate the accuracy of the method, the maximum absolute errors are defined by

$$\|E_U\| = \max_{-N-2 \le j \le N+2} \{U_0 |U_c(z_j) - U(z_j)|\},$$

$$\|E_V\| = \max_{-N-2 \le j \le N+2} \{U_0 |V_c(z_j) - V(z_j)|\},$$

and

$$\|E_W\| = max\{\|E_U\|, \|E_V\|\}, \tag{53}$$

where the units are ms^{-1}.

Example 1.(seabed linear stress condition)
To keep the parameters and variables identical to those in [18], [19], [32], we choose $\chi = 45^\circ$, the linear stress condition at the seabed, $\sigma = 0.1$, $D_0 = 100$ m, $D_E = 20$ and $\kappa = 5$. In this example we solve a discrete system of size $(m \times m)$ given by (46), where $m = 2N + 5$. To demonstrate the numerical convergence of the method we repeat the process for N=4,8,...,64. The errors are listed in Table I and exhibit a very high degree of accuracy.

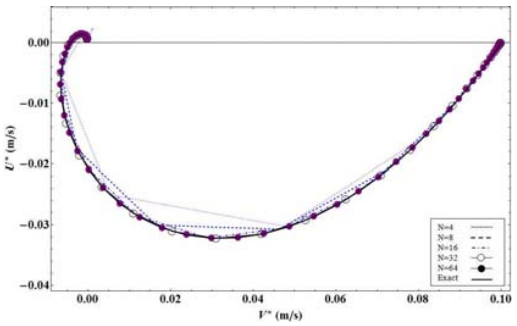

Fig. 2. The Sinc-Collocation Ekman Spiral projection of Example 1 for different values of N against the exact solution while $\sigma = 0.1, \chi = 45, \kappa = 5, D_0 = 100\ m, D_E = 20\ m$.

In Figure 2, we depict the exponential convergence of the solutions by the horizontal projection of the Ekman spiral (HPES). Our solution for N=64, has a high degree of accuracy which makes it hard for us to distinguish it from the exact solution.

In Table II, we exhibit the comparison we made between our findings and those in papers [18], [32]. E_W, E_2 and E_3 convey the maximum errors of our method, the one in [18] and [32] respectively.

TABLE II
A COMPARISON BETWEEN THE ERRORS IN EXAMPLE 1 AND THOSE IN PAPERS [18], [32], WHILE $\sigma = 0.1, \chi = 45^\circ, \kappa = 5, D_0 = 100\ m$ AND $D_E = 20\ m$.

N	m	h	$\|E_W\|$	$\|E_2\|$	$\|E_3\|$
4	13	0.3163	3.47×10^{-3}	1.10×10^{-3}	5.38×10^{-2}
8	21	0.2015	1.26×10^{-4}	2.50×10^{-4}	4.57×10^{-2}
16	37	0.1224	2.49×10^{-6}	2.76×10^{-5}	1.86×10^{-2}
32	69	0.0720	2.96×10^{-8}	8.99×10^{-7}	8.19×10^{-3}
64	133	0.0414	1.82×10^{-10}	5.78×10^{-9}	7.13×10^{-4}

TABLE III
ERRORS OF EXAMPLE 2 (CONSTANT EDDY VISCOSITY) WHILE $\sigma = 0, \chi = 45^\circ, \kappa = 5, D_0 = 100\ m$ AND $D_E = 20\ m$.

N	m	h	$\|E_U\|$	$\|E_V\|$	$\|E_W\|$
4	13	0.3163	3.06×10^{-3}	3.38×10^{-3}	3.38×10^{-3}
8	21	0.2015	1.25×10^{-4}	8.42×10^{-5}	1.25×10^{-4}
16	37	0.1224	2.48×10^{-6}	1.23×10^{-6}	2.48×10^{-6}
32	69	0.0720	2.95×10^{-8}	1.43×10^{-8}	2.95×10^{-8}
64	133	0.0414	8.26×10^{-11}	8.37×10^{-11}	8.37×10^{-11}

Example 2.(No-slip condition at the seabed)
In this example, we assume $\sigma = 0$ and all other parameters similar to Example 1. The absolute errors of our solutions are listed in Table III and a very close similarity to those in Example 1 is explored. The HPES for different values of N, against the exact solution are portrayed in Figure 3. Likewise, Table IV provides the maximum errors of our method, and those in [18], [32] respectively.

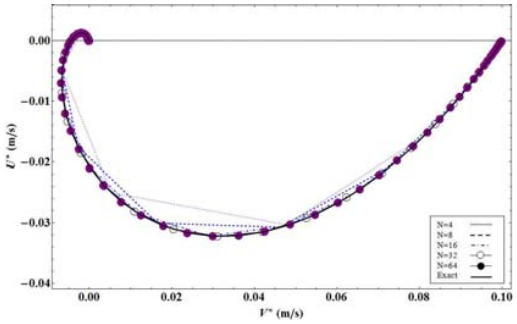

Fig. 3. The Sinc-Collocation Ekman Spiral projection of Example 2 for different values of N against the exact solution while $\sigma = 0, \chi = 45, \kappa = 5, D_0 = 100\ m, D_E = 20\ m$.

B. Variable Eddy Viscosity

In the real world the eddy viscosity is a depth- and time-dependent variable. In this paper, we specifically study the depth-dependent eddy viscosity. Likewise, we study a specific

TABLE IV
A COMPARISON BETWEEN THE ERRORS IN EXAMPLE 2 AND THOSE IN PAPERS [18], [32], WHILE $\sigma = 0, \chi = 45^\circ, \kappa = 5, D_0 = 100\ m$ AND $D_E = 20\ m$.

N	m	h	$\|E_W\|$	$\|E_2\|$	$\|E_3\|$
4	13	0.3163	3.38×10^{-3}	1.10×10^{-3}	5.33×10^{-2}
8	21	0.2015	1.25×10^{-4}	2.48×10^{-4}	4.55×10^{-2}
16	37	0.1224	2.48×10^{-6}	2.75×10^{-5}	1.85×10^{-2}
32	69	0.0720	2.95×10^{-8}	8.96×10^{-7}	8.17×10^{-3}
64	133	0.0414	8.37×10^{-11}	5.76×10^{-9}	7.1×10^{-4}

case of time-dependent eddy viscosity in which when $t \to \infty$, it can be considered as a constant.

In seas of shallow to intermediate depth, the eddy viscosity has the maximum values of ${A^*}_v(z^*)$ at the intermediate depths and the minimum values near the surface and seabed. But in deeper seas, it is expected that ${A^*}_v(z^*)$ has the maximum values near the surface and its value decreases going towards the seabed. The latter case is illustrated by

$$ {A^*}_v(z^*) = 0.02[1 - (0.0075)z^*]^2,\ 0 < z^* < D_0. \quad (54) $$

which decreases quadratically from the value of 0.02 $m^2\ s^{-1}$ to the minimum value of 0.00125 $m^2\ s^{-1}$. The eddy viscosity in the first case, follows a quadratic model given by

$$ {A^*}_v(z^*) = 0.02[1 + (0.12)z^*(1 - (0.01)z^*)],\ 0 < z^* < D_0. \quad (55) $$

increasing from the initial value of 0.02 $m^2 s^{-1}$ to the peak value of 0.08 and then decreasing to 0.02 $m^2\ s^{-1}$.

Example 3.(The decreasing eddy viscosity)
In this example, we find the approximate solutions $U_c(z)$ and $V_c(z)$ via the complex velocity discrete system while the variable eddy viscosity is given by (54). The parameters are chosen identical to those in Example 1. Since there is not any closed form solution of this case, we depict the HPES of decreasing eddy viscosity against that of constant eddy viscosity for different values of N in Figure 4.

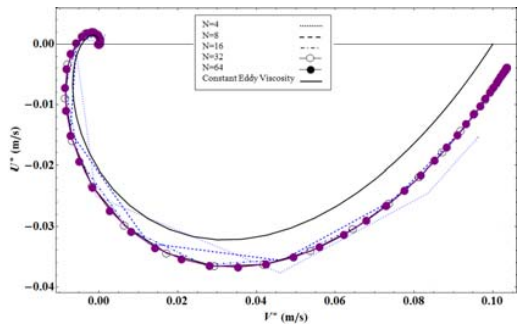

Fig. 4. The Sinc-Collocation Ekman Spiral projection of Example 3 for different values of N against the exact solution of the constant eddy viscosity case while $\sigma = 0.1, \chi = 45, \kappa = 5, D_0 = 100\ m, D_E = 20\ m$.

Example 4. (The quadratic eddy viscosity)
This example is similar to Example 3, but the eddy viscosity is given by (55). Since no exact solution for this case is reported, we portray the HPES of quadratic eddy viscosity for different values of N, against that of constant eddy viscosity in Figure 5.

Example 5. (A steady-state problem with a no-slip bottom condition)
In realistic oceanography problems, eddy viscosity is a function of depth and time. Field studies show that the value of eddy viscosity near the surface is dependent to the wind stress which relies on time. Therefore, in shallow seas ($D_0 < 100\ m$), the eddy viscosity is assumed dependent of time but independent of depth. There is an interesting example of this case studied in below.

Assume the non-dimensional time-dependent eddy viscosity $A_v(t) = 4 - 3e^{-t}$. At the steady-state condition ($t \to \infty$), it will be equivalent to $A_\infty \equiv 4$. This example is similar to Example 2, in which the eddy viscosity is constant. Consider the steady-state boundary value problem

$$ A_\infty \frac{d^2w(z)}{dz^2} + 2\kappa^2 i w(z) = -2\kappa^3 i \left(\frac{1-z}{A_\infty}\right) e^{i\chi} \quad (56) $$

with time-independent BCs

$$ \frac{dw(0)}{dz} = 0, \quad (57) $$

$$ w(1) = 0. \quad (58) $$

and the no-slip boundary condition $\sigma = 0$.

The exact solution of this problem is $W(z) = U_0(U(z) + iV(z))$ where U(z) and V(z) are given by

$$ U(z) = R(W_c(z))\cos(\chi) - I(W_c(z))\sin(\chi), $$

$$ V(z) = R(W_c(z))\sin(\chi) - I(W_c(z))\cos(\chi). $$

and

$$ W_c(z) = \left(\frac{1+i}{2}\right) \frac{\sinh\left((1-i)\kappa(1-z)\sqrt{\frac{1}{A_\infty}}\right)}{\sqrt{A_\infty}\cosh\left((1-i)\kappa\sqrt{\frac{1}{A_\infty}}\right)} \quad (59) $$

The results comparing to the exact solution is depicted in Table V. Figure 6, displays the HPES of the current problem for N = 4,8,...,64 against the exact solution. In Table VI, we compare our results to those in [32].

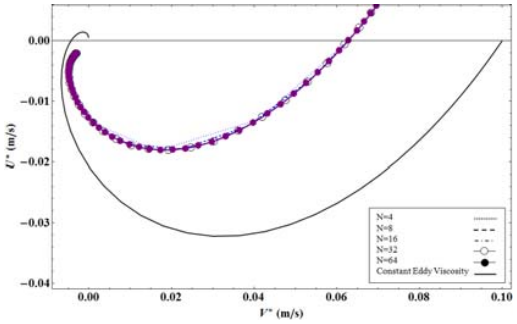

Fig. 5. The Sinc-Collocation Ekman Spiral projection of Example 4 for different values of N against the exact solution of the constant eddy viscosity case while $\sigma = 0.1, \chi = 45, \kappa = 5, D_0 = 100\ m, D_E = 20\ m$.

TABLE V
ERRORS OF EXAMPLE 5 (TIME-DEPENDENT EDDY VISCOSITY IN THE COMPLEX SYSTEM) WHILE $\sigma = 0, \chi = 45°, \kappa = 3.14, D_0 = 60\ m$ AND $D_E = 19\ m$.

N	m	h	$\|E_U\|$	$\|E_V\|$	$\|E_W\|$
4	13	0.316	2.00×10^{-4}	8.58×10^{-5}	2.00×10^{-4}
8	21	0.201	4.59×10^{-7}	6.78×10^{-7}	6.78×10^{-7}
16	37	0.122	1.45×10^{-7}	6.00×10^{-8}	1.46×10^{-7}
32	69	0.072	1.74×10^{-9}	7.15×10^{-10}	1.74×10^{-9}
64	133	0.041	3.94×10^{-11}	8.03×10^{-11}	8.03×10^{-11}

V. CONCLUSION

In this paper, we applied a Sinc-Collocation approach developed by Abdella [30] to numerically approximate the solution of a 3D oceanography model observed in [18]. The validity, stability and accuracy of our approach is examined by solving

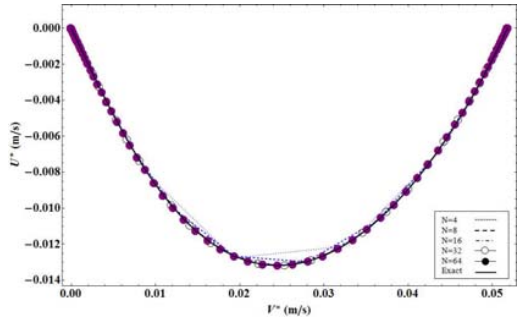

Fig. 6. The Sinc-Collocation Ekman Spiral projection of Example 5 for different values of N against the exact solution while $\sigma = 0, \chi = 45, \kappa = 3.14, D_0 = 60\ m, D_E = 19\ m$.

TABLE VI
A COMPARISON BETWEEN THE ERRORS IN EXAMPLE 5 AND THOSE IN PAPER [32], WHILE $\sigma = 0, \chi = 45°, \kappa = 3.14, D_0 = 60\ m$ AND $D_E = 19\ m$.

N	m	h	$\|E_W\|$	$\|E_3\|$
4	13	0.3163	2.00×10^{-4}	2.13×10^{-1}
8	21	0.2015	6.78×10^{-7}	2.74×10^{-1}
16	37	0.1224	1.46×10^{-7}	8.61×10^{-2}
32	69	0.0720	1.74×10^{-9}	2.26×10^{-2}

several examples found in [18], [32] and comparing the results with the exact solutions and those in prior studies. Our results show that the presented Sinc-Collocation approach is very promising in oceanographic problems. In Particular, we would claim that the Sinc-Collocation method is superior to the Galerkin version due to its simple implementation and higher accuracy. As expected, the errors of our method exponentially converges to zero depending on the values of N. In closing, we would claim that the current method is eligible to be a proper alternative to other methods which have been used thus far.

Future research may include an investigation of the model with the time-dependent eddy viscosity which leads to solving partial differential equations using the approach discussed in this paper.

REFERENCES

[1] M. A. Noor and E. Al-Said, "Finite-difference method for a system of third-order boundary-value problems," *Journal of optimization theory and applications*, vol. 112, no. 3, pp. 627–637, 2002.
[2] O. Axelsson and V. A. Barker, *Finite element solution of boundary value problems: theory and computation*. Society for Industrial and Applied Mathematics, 1987, vol. 35.
[3] Z. Csendes, "A novel finite element method for two-point boundary value problems," *Mathematics and Computers in Simulation*, vol. 20, no. 3, pp. 197–203, 1978.
[4] K. Ruotsalainen and W. Wendland, "On the boundary element method for some nonlinear boundary value problems," *Numerische Mathematik*, vol. 53, no. 3, pp. 299–314, 1988.
[5] B. S. Attili and M. I. Syam, "Efficient shooting method for solving two point boundary value problems," *Chaos, Solitons & Fractals*, vol. 35, no. 5, pp. 895–903, 2008.
[6] J. Rashidinia and M. Ghasemi, "B-spline collocation for solution of two-point boundary value problems," *Journal of computational and applied mathematics*, vol. 235, no. 8, pp. 2325–2342, 2011.
[7] F. Stenger, "Summary of sinc numerical methods," *Journal of Computational and Applied Mathematics*, vol. 121, no. 1, pp. 379–420, 2000.
[8] F. Keinert, "Uniform approximation to x β by sinc functions," *Journal of approximation theory*, vol. 66, no. 1, pp. 44–52, 1991.
[9] S. Narasimhan, J. Majdalani, and F. Stenger, "A first step in applying the sinc collocation method to the nonlinear navier-stokes equations," *Numerical Heat Transfer: Part B: Fundamentals*, vol. 41, no. 5, pp. 447–462, 2002.
[10] A. Lippke, "Analytical solutions and sinc function approximations in thermal conduction with nonlinear heat generation," *Journal of Heat Transfer (Transcations of the ASME (American Society of Mechanical Engineers), Series C);(United States)*, vol. 113, no. 1, 1991.
[11] K. Al-Khaled, "Numerical approximations for population growth models," *Applied mathematics and computation*, vol. 160, no. 3, pp. 865–873, 2005.
[12] J. Lund and C. R. Vogel, "A fully-galerkin method for the numerical solution of an inverse problem in a parabolic partial differential equation," *Inverse Problems*, vol. 6, no. 2, p. 205, 1999.
[13] R. C. Smith and K. L. Bowers, "Sinc-galerkin estimation of diffusivity in parabolic problems," *Inverse problems*, vol. 9, no. 1, p. 113, 1999.
[14] K. Parand and A. Pirkhedri, "Sinc-collocation method for solving astrophysics equations," *New Astronomy*, vol. 15, no. 6, pp. 533–537, 2010.
[15] M. El-Gamel and A. Zayed, "Sinc-galerkin method for solving nonlinear boundary-value problems," *Computers & Mathematics with Applications*, vol. 48, no. 9, pp. 1285–1298, 2004.
[16] F. Stenger and M. J. O'Reilly, "Computing solutions to medical problems via sinc convolution," *Automatic Control, IEEE Transactions on*, vol. 43, no. 6, pp. 843–848, 1998.
[17] K. Abdella, X. Yu, and I. Kucuk, "Application of the sinc method to a dynamic elasto-plastic problem," *Journal of Computational and Applied Mathematics*, vol. 223, no. 2, pp. 626–645, 2009.
[18] D. Winter, K. L. Bowers, and J. Lund, "Wind-driven currents in a sea with a variable eddy viscosity calculated via a sinc–galerkin technique," *International journal for numerical methods in fluids*, vol. 33, no. 7, pp. 1041–1073, 2000.
[19] S. Koonprasert and K. L. Bowers, "Block matrix sinc-galerkin solution of the wind-driven current problem," *Applied mathematics and computation*, vol. 155, no. 3, pp. 607–635, 2004.
[20] E. Hesameddini and E. Asadolahifard, "The sinc-collocation method for solving the telegraph equation," *Journal of Computer Engineering and Informatics*.
[21] A. Saadatmandi, "Numerical study of second painlevé equation," *Communications in Numerical Analysis*, vol. 2012, 2012.
[22] B. Bialecki, "Sinc-collection methods for two-point boundary value problems," *IMA Journal of Numerical Analysis*, vol. 11, no. 3, pp. 357–375, 1991.
[23] V. W. Ekman, "On the influence of the earth\'s rotation on ocean currents," *Ark. Mat. Astron. Fys.*, vol. 2, pp. 1–53, 1905.
[24] N. Heaps *et al.*, "On the numerical solution of the three-dimensional hydrodynamical equations for tides and storm surges," *Mémoires de la Société Royale des Sciences de Liège. Sixième Série*, 1972.
[25] N. Heaps, "Three-dimensional model for tides and surges with vertical eddy viscosity prescribed in two layersi. mathematical formulation," *Geophysical Journal of the Royal Astronomical Society*, vol. 64, no. 1, pp. 291–302, 1981.
[26] R. Lardner and Y. Song, "A hybrid spectral method for the three-dimensional numerical modelling of nonlinear flows in shallow seas," *Journal of Computational Physics*, vol. 100, no. 2, pp. 322–334, 1992.
[27] A. Davies, "The numerical solution of the three-dimensional hydrodynamic equations, using a b-spline representation of the vertical current profile," *Elsevier Oceanography Series*, vol. 19, pp. 1–25, 1977.
[28] A. Davies and A. Owen, "Three dimensional numerical sea model using the galerkin method with a polynomial basis set," *Applied mathematical modelling*, vol. 3, no. 6, pp. 421–428, 1979.
[29] A. M. Davies, "Solution of the 3d linear hydrodynamic equations using an enhanced eigenfunction approach," *International journal for numerical methods in fluids*, vol. 13, no. 2, pp. 235–250, 1991.
[30] K. Abdella, "Numerical solution of two-point boundary value problems using sinc interpolation," in *Proceedings of the American Conference on Applied Mathematics (American-Math'12): Applied Mathematics in Electrical and Computer Engineering*, 2012, pp. 157–162.
[31] R. Burden and J. Faires, "Numerical analysis 7th ed., brooks/cole, thomson learning," 2001.
[32] S. Koonprasert, "The sinc-galerkin method for problems," Ph.D. dissertation, MONTANA STATE UNIVERSITY Bozeman, 2003.